AAS 11-644

A COMPARISON OF FIXED-TERMINAL DIRECTION GUIDANCE LAWS FOR SPACECRAFT RENDEZVOUS

Renato Zanetti* **and Fred D. Clark†**

This work examines and compares two fixed-terminal direction guidance laws to rendezvous with a target in circular orbit. Both laws exactly satisfy the constraint. The first algorithm is based on the optimization of a quadratic performance index. The second algorithm has as many constraints as degrees of freedom and is the guidance law utilized by the Space Shuttle. Similarities and differences between the two approaches are discussed and numerical simulations are presented.

INTRODUCTION

Many space applications involve rendezvous with a vehicle in circular orbit. A subset of these applications requires the visiting vehicle to approach with a constant direction as seen by the target. This is the case for vehicles approaching the International Space Station (ISS), for example. By approaching it in a straight line the crew onboard the station can easily monitor non-nominal situations. The Space Shuttle carries a rendezvous and proximity operations program (RPOP) [1] that employs a straight-line guidance law called glideslope [2]. Vehicles visiting the ISS usually employ a fixed direction terminal approach, including the H-II transfer vehicle (HTV) [3], the automated transfer vehicle (ATV) [4], and Cygnus [5]. In this work an optimal constant direction guidance law to rendezvous with a target in circular orbit is presented and compared to the RPOP guidance.

Much work exists in the general area of optimal space trajectories; an illustrative early work is that by Lawden [6]. Carter studied minimum delta-v maneuvers to rendezvous with a vehicle in circular orbit [7]. The approach used by Carter and by many authors after him is to optimize the system subject to the linearized dynamics, the so-called Clohessy-Wiltshire equations [8]. The rendezvous strategy by Lembeck and Prussing [9] is to add to an initial impulsive phase a low-thrust phase. Since continuous thrust is necessary to guide on the glideslope, this work also assumes low-thrust propulsion.

Various aspects of this problem were generalized. Carter and Humi study the impulsive rendezvous in proximity of a general Keplerian orbit [10] while Carter studies the continuous thrust case [11]. Power limitations and thrust bounds are also studied [12]. Guelman and Aleshin [13] develop a two-stage solution for the fixed terminal-approach direction. The first stage consists of an unconstrained optimization that puts the vehicle on the glideslope. The second stage is along the glideslope. In this work only the terminal phase is considered, when the spacecraft is required to fly on the glideslope.

*Senior Member of the Technical Staff, Vehicle Dynamics and Controls, The Charles Stark Draper Laboratory, 17629 El Camino Real, Suite 470, Houston, Texas, 77058. rzanetti@draper.com

†Principal Member of the Technical Staff, Vehicle Dynamics and Controls, The Charles Stark Draper Laboratory, 17629 El Camino Real, Suite 470, Houston, Texas, 77058. fclark@draper.com

The laws compared in this work differ considerably from the work of Guelman and Aleshin. In their work the constraint is not enforced directly, but the squared distance to the glideslope is added to the performance index with a weighting parameter. The bigger the parameter the closer the constraint is to be satisfied. In this work the constraint is satisfied exactly. Another difference between the two works is that Guelman and Aleshin solve their optimization numerically, while closed-form solutions are used in this paper.

RPOP REFERENCE TRAJECTORY

The RPOP reference trajectory is recalculated by the guidance algorithm at each call. It is assumed that the desired out-of-plane component is zero. Clohessy-Wiltshire (CW) equations are used to express the dynamics of the chaser vehicle in proximity of a target in circular orbit. The local vertical-local horizontal (LVLH) frame used in this derivation is centered at the target, has the x-axis along the velocity vector and the z-axis along the radial direction pointing down. In this coordinate system the linearized equations of relative motion are given by

$$\ddot{x} = 2\omega\dot{z} + u_x \tag{1}$$

$$\ddot{y} = -\omega^2 y + u_y \tag{2}$$

$$\ddot{z} = 3\omega^2 z - 2\omega\dot{x} + u_z, \tag{3}$$

these equations are valid when x, y, and z are CG-to-CG coordinates. The control acceleration is given by $\mathbf{u} = [u_x \quad u_y \quad u_z]^{\mathrm{T}}$, and ω is the orbital angular velocity of the target. Since the out-of-plane component is assumed to be zero its corresponding equation is neglected in calculating the reference trajectory.

The chaser CG-to-target CG distance, $\mathbf{r}_{ccg/tcg}$, is written in terms of the target docking port to Chaser docking port distance, $\mathbf{r}_{cdp/tdp}$, as

$$\mathbf{r}_{ccg/tcg} = \mathbf{r}_{cdp/tdp} + \mathbf{r}_{cdp/ccg} - \mathbf{r}_{tdp/tcg} = \mathbf{r}_{cdp/tdp} + \mathbf{r}_{offset}. \tag{4}$$

The glideslope angle θ is defined as the angle between the direction of the approach and the positive x-axis, counted positive using the right-hand rule around the negative y-axis. The direction along the line of approach is called radial r, and its in-plane perpendicular is called transversal t. Assuming a constant relative attitude the derivative of $\mathbf{r}_{offset}$ is zero and we have that

$$x_{ccg/tcg} = r\cos\theta - t\sin\theta + x_{offset} \tag{5}$$

$$z_{ccg/tcg} = r\sin\theta + t\cos\theta + z_{offset} \tag{6}$$

$$u_x = \cos\theta u_r - \sin\theta u_t \tag{7}$$

$$u_z = \cos\theta u_t + \sin\theta u_r. \tag{8}$$

Since the transversal distance between docking ports is constant and equal to zero, the CW equations can be rewritten as

$$u_t = 2\omega\dot{r} - 3\omega^2\cos\theta(r\sin\theta + z_{offset}) \tag{9}$$

$$u_r = \ddot{r} - 3\omega^2\sin\theta(r\sin\theta - z_{offset}) \tag{10}$$

A requirement of the Shuttle reference trajectory is that minimum or no plume impingement of the target should occur. To meet this requirement the vehicle needs to thrust only along the transversal

direction. The RPOP algorithm includes an additional parameter that represents the canting of the Space Shuttle's jet. This parameter is needed when the $\Delta\mathbf{v}$ obtaned is biased with respect to the commanded $\Delta\mathbf{v}$. For the purpose of this discussion the canting angle is unnecessary and assumed to be zero.

Assuming no thrust in the radial direction Eq. (10) becomes

$$\ddot{r} - 3\omega^2 r \sin^2\theta = 3\omega^2 z_{offset} \sin\theta. \tag{11}$$

assuming $\sin\theta \neq 0$ the solution of Eq. (11) is given by

$$r = c_1 \cosh(mt) + c_2 \sinh(mt) + c_3, \tag{12}$$

where

$$m = \sqrt{3}(\sin\theta)\omega \tag{13}$$
$$c_1 = r_0 - c_3 \tag{14}$$
$$c_2 = \frac{\dot{r}_0}{m} \tag{15}$$
$$c_3 = \frac{-z_{offset}}{\sin\theta}. \tag{16}$$

For a given initial range and range rate, the trajectory is completely determined. The initial range is given while the initial rate is obtained by back-propagating from the desired final condition. At the final time we have that

$$r_f = c_1 \cosh(mt_f) + \frac{\dot{r}_0}{m} \sinh(mt_f) + c_3 \tag{17}$$
$$\dot{r}_f = c_1 m \sinh(mt_f) + \dot{r}_0 \cosh(mt_f), \tag{18}$$

therefore $\dot{r}_0$ must satisfy

$$\dot{r}_0 = m\frac{r_f - c_3 - c_1\cosh(mt_f)}{\sinh(mt_f)} \tag{19}$$

and

$$\dot{r}_0 = \frac{\dot{r}_f - mc_1 \sinh(mt_f)}{\cosh(mt_f)}, \tag{20}$$

or

$$(r_f - c_3)\cosh(mt_f) = \frac{\dot{r}_f}{m}\sinh(mt_f) + c_1, \tag{21}$$

the final time can be found solving for t_f in Eq. (21). RPOP solves the non-zero canting angle case of Eq. (21) using the Newton-Raphson method. For the zero canting angle case an analytical solution exist and is given by

$$t_f = \begin{cases} [\sinh^{-1}(-mr_0\cosh\phi/\dot{r}_f) - \phi]/m, & \phi = \tanh^{-1}(-mr_f/\dot{r}_f) & \text{if } |mr_f/\dot{r}_f| < 1 \\ [\cosh^{-1}(r_0/r_f)]/m, & r_f \neq 0 & \text{if } \dot{r}_f = 0 \\ [\cosh^{-1}(-mr_0\sinh\phi/\dot{r}_f) - \phi]/m, & \phi = \tanh^{-1}[-\dot{r}_f/(m\dot{r}_f)] & \text{if } |mr_f/\dot{r}_f| > 1 \end{cases} \tag{22}$$

Substituting t_f into either of Eqs. (19) or (20) the initial rate can be found.

For V-bar approaches $\sin\theta = 0$ and Eq. (11) reduces to

$$\ddot{r} = 0 \tag{23}$$

which is a constant relative velocity approach with solution

$$r = r_0 + \dot{r}_f t, \tag{24}$$

therefore a closing final rate is necessary for a solution to exist.

Since the Space Shuttle employs large thrusters and almost impulsive maneuvers the commanded trajectory is not the nominal trajectory. Instead a targeting algorithm is called at fixed intervals, typically one to three minutes. An impulsive maneuver is computed such that the vehicle is placed on the nominal trajectory the next time the targeting algorithm is called.

OPTIMAL GUIDANCE

For a non-impulsive, power limited propulsion system, an appropriate performance index is (see for example [14] and citations therein)

$$\mathcal{J} = \frac{1}{2}\int_0^{t_f} \mathbf{u}^{\mathrm{T}}\mathbf{u}\, dt, \tag{25}$$

subject to the linear dynamics governed by the CW equations and constrained to be on the glideslope. The performance index of Eq. (25) is particularly useful for continuous low-thrust systems; for impulsive maneuvers a minimum delta-v solution is more appropriate. To remain on the glideslope at all times it is necessary to continuously thrust in the direction perpendicular to the glideslope. For electric propulsion systems Eq. (25) is also a minimum fuel solution. For any thruster the expelled mass is given by

$$\dot{m}_e = \frac{T}{I_{sp}\, g_0}, \tag{26}$$

where T is the desired thrust magnitude and g_0 is constant. For an electric thruster the specific impulse is given by

$$I_{sp} = \frac{2P}{g_0 T}, \tag{27}$$

where P is the output power. The input electrical power is greater than P and depends on the efficiency of the thruster. While the output power is not always constant with a throttleable engine, for the purpose of this work it is assumed it is. By combining the last two equations it results that the total expelled mass is proportional to the square of the thrust

$$\dot{m}_e = \frac{T^2}{2P}. \tag{28}$$

For low thrust vehicles when the expelled mass is negligible with respect to the total mass it follows that the expelled mass is proportional to the square of the commanded acceleration.

In the glideslope frame the equations of motion are

$$\ddot{r} = 2\omega\dot{t} + 3\omega^2 r\sin^2\theta + 3\omega^2 t\sin\theta\cos\theta + u_r \tag{29}$$

$$\ddot{t} = -2\omega\dot{r} + 3\omega^2 r\sin\theta\cos\theta + 3\omega^2 t\cos^2\theta + u_t \tag{30}$$

$$\ddot{y} = -\omega^2 y + u_y, \tag{31}$$

where zero offset is assumed. In order to approach the target in a straight line it is necessary that $t = \dot{t} = \ddot{t} = 0$, hence

$$\ddot{r} = 3\omega^2 r \sin^2\theta + u_r \tag{32}$$

$$0 = -2\omega\dot{r} + 3\omega^2 r \sin\theta\cos\theta + u_t \tag{33}$$

$$\ddot{y} = -\omega^2 y + u_y, \tag{34}$$

it follows that the optimal transversal acceleration is given by

$$u_t^* = 2\omega\dot{r} - 3\omega^2 r \sin\theta\cos\theta. \tag{35}$$

It is assumed that the desired approach direction lies in the plane of motion of the target's vehicle. Most vehicles employ the strategy of eliminating the out-of-plane component early in the rendezvous phase. Since the in and out-of-plane dynamics are decoupled from each other, the residual out-of-plane error can be controlled independently. The performance index to be minimized becomes

$$\mathcal{J} = \frac{1}{2}\int_0^{t_f} [u_r^2 + u_t^2]dt = \frac{1}{2}\int_0^{t_f} [u_r^2 + (2\omega\dot{r} - 3\omega^2 r \sin\theta\cos\theta)^2]dt \tag{36}$$

subject to the kinematic constraint

$$\dot{r} = v \tag{37}$$

$$\dot{v} = 3\omega^2 r \sin^2\theta + u_r, \tag{38}$$

and the boundary conditions

$$r(0) = r_0 \qquad r(t_f) = r_f \qquad v(0) = v_0 \qquad v(t_f) = v_f. \tag{39}$$

The Hamiltonian is given by

$$H = \frac{1}{2}[u_r^2 + (2\omega\dot{r} - 3\omega^2 r \sin\theta\cos\theta)^2] + \lambda_r v + \lambda_v(3\omega^2 r \sin^2\theta + u_r), \tag{40}$$

the costate equations are given by

$$\dot{\lambda}_r = -\frac{\partial H}{\partial r} = -(2\omega\dot{r} - 3\omega^2 r \sin\theta\cos\theta)(-3\omega^2 \sin\theta\cos\theta) - 3\omega^2 \sin^2\theta\lambda_v \tag{41}$$

$$\dot{\lambda}_v = -\frac{\partial H}{\partial v} = -2\omega(2\omega\dot{r} - 3\omega^2 r \sin\theta\cos\theta) - \lambda_r \tag{42}$$

and the control optimality condition is given by

$$\frac{\partial H}{\partial u_r} = 0 = u_r + \lambda_v. \tag{43}$$

Therefore the optimal control is given by $u_r = -\lambda_v$ and augmenting states and costates in a single vector it follows that

$$\frac{d}{dt}\begin{bmatrix} r \\ v \\ \lambda_r \\ \lambda_v \end{bmatrix} = \frac{d}{dt}\mathbf{x} = \mathbf{A}\mathbf{x}, \tag{44}$$

where

$$\mathbf{A} = \begin{bmatrix} 0 & 1 & 0 & 0 \\ 3\omega^2 \sin^2\theta & 0 & 0 & -1 \\ -9\omega^4 \sin^2\theta \cos^2\theta & 6\omega^3 \sin\theta\cos\theta & 0 & -3\omega^2 \sin^2\theta \\ 6\omega^3 \sin\theta\cos\theta & -4\omega^2 & -1 & 0 \end{bmatrix}. \tag{45}$$

Partitioning the state transition matrix of $\mathbf{A}$ in four 2-by-2 blocks

$$\mathbf{\Phi}_{\mathbf{A}}(\tau, t_0) = e^{\mathbf{A}(\tau - t_0)} = \begin{bmatrix} \mathbf{\Phi}_{rr}(\tau - t_0) & \mathbf{\Phi}_{r\lambda}(\tau - t_0) \\ \mathbf{\Phi}_{\lambda r}(\tau - t_0) & \mathbf{\Phi}_{\lambda\lambda}(\tau - t_0) \end{bmatrix} \tag{46}$$

the initial values of the costates are determined to be

$$\begin{bmatrix} \lambda_r(t_0) \\ \lambda_v(t_0) \end{bmatrix} = \mathbf{\Phi}_{r\lambda}^{-1}(t_f - t_0) \left(\begin{bmatrix} r_f \\ v_f \end{bmatrix} - \mathbf{\Phi}_{rr}(t_f - t_0) \begin{bmatrix} r_0 \\ v_0 \end{bmatrix} \right), \tag{47}$$

and the optimal control history is given by

$$u_r^*(t) = \begin{bmatrix} 0 & 0 & 0 & -1 \end{bmatrix} \mathbf{\Phi}_{\mathbf{A}}(t, t_0)\, \mathbf{x}(t_0). \tag{48}$$

To show that the solution is a minimum the Weierstrass and Legendre-Clebsch conditions are tested [15]. The Weierstrass condition requires that the Hamiltonian evaluated at any admissible comparison control u_r is larger than the Hamiltonian evaluated at the optimal control u_r^*. From Eq. (40)

$$H(u_r) - H(u_r^*) = [0.5u_r^2 + \lambda_v u_r - 0.5(u_r^*)^2 - \lambda_v u_r^*], \tag{49}$$

substituting $\lambda_v = -u_r^*$

$$H(u_r) - H(u_r^*) = \frac{1}{2}(u_r - u_r^*)^2 \geq 0, \tag{50}$$

therefore the Weierstrass condition is satisfied.

The Legendre-Clebsch condition requires that the second order partial of the Hamiltonian with respect to the optimal control is positive definite. From Eq. (40)

$$\frac{\partial^2 H}{\partial u_r^2} = 1, \tag{51}$$

hence the Legendre-Clebsch condition is also satisfied and the solution is indeed a minimum.

IMPLEMENTATION CONSIDERATIONS

The most computationally demanding part of the algorithm is the computation of the matrix exponential in order to obtain the state transition matrix. However, applying the Cayley-Hamilton theorem vastly reduces the complexity. The matrix exponential of the 4-by-4 matrix $\mathbf{A}$ can be computed as

$$e^{\mathbf{A}\Delta t} = \sum_{k=0}^{3} \alpha_k \mathbf{A}^k, \tag{52}$$

where the coefficients α_k are calculated solving

$$e^{\lambda_i \Delta t} = \sum_{k=0}^{3} \alpha_k \lambda_i^k, \tag{53}$$

where λ_i is the ith eigenvalue of $\mathbf{A}$.

Since $\mathbf{A}$ is constant, so are its four eigenvalues, which can be computed *a priori* and are given by

$$\lambda_i = \pm \left(3\sin^2\theta + 2 \pm \sqrt{9\sin^4\theta + 3\sin^2\theta + 4}\right)^{1/2} \omega. \tag{54}$$

Using vector notation

$$\boldsymbol{\lambda} = \begin{bmatrix}\lambda_1 & \lambda_2 & \lambda_3 & \lambda_4\end{bmatrix}^{\mathrm{T}} \qquad \boldsymbol{\alpha} = \begin{bmatrix}\alpha_0 & \alpha_1 & \alpha_2 & \alpha_3\end{bmatrix}^{\mathrm{T}} \tag{55}$$

it follows that

$$\boldsymbol{\alpha} = \boldsymbol{\Lambda}^{-1} e^{\boldsymbol{\lambda}\Delta t}, \tag{56}$$

where $e^{\mathbf{w}}$ represents a vector whose components are the exponentials of the components of vector $\mathbf{w}$. The four columns of $\boldsymbol{\Lambda}$ are given by the eigenvalues elevated to the zeroeth, first, second, and third power, respectively. The inverse of $\boldsymbol{\Lambda}$ needs to be computed only once and can be a parameter uploaded from the ground.

A practical implementation should not assume that t, z and their derivatives are always zero but dispersions should be corrected. An inner loop controller needs to be implemented to cancel the out-of-plane and transversal components. Alternatively the control thrust can be chosen using a simple PD controller

$$u_r = u_r^* - 2\omega\dot{t} - 3\omega^2 \sin\theta\cos\theta t \tag{57}$$

$$u_t = u_t^* - 3\omega^2\cos^2\theta t - k_p t - k_d\dot{t} \tag{58}$$

$$u_y = -k_y\dot{y}. \tag{59}$$

where the asterisk represents the previously defined values from the guidance law. The positive coefficients k_p, k_d, and k_y are design parameters to dampen the dispersions.

THREE SPECIAL CASES

Three scenarios deserve special attention, these cases are the common glideslope angles that possess an analytic solution. These cases are the V-bar approach ($\theta = 0$) in which the chaser starts directly in front of the target, the minus V-bar approach ($\theta = \pi$) in which the chaser starts directly behind the target, and the R-bar approach ($\theta = \pi/2$) in which the chaser starts directly below the target. A minus R-bar approach also possesses an analytical solution, but in practice this kind of approach is not used very often.

The V-bar approach is the most common Space Shuttle rendezvous strategy. Eq. (54) shows that $\mathbf{A}$ has repeated eigenvalues only when $\sin\theta = 0$. Under this circumstance the repeated eigenvalues are equal to zero and the other two are given by $\pm 2\omega$. The system of Eq. (53) is not solvable in this situation, the equation relative to the repeated eigenvalue needs to be replaced by its derivative

$$\lambda_i\, e^{\lambda_i \Delta t} = \sum_{k=1}^{3} \alpha_k \lambda_i^{k-1}. \tag{60}$$

Solving this modified set of equations results in

$$\alpha_0 = 1 \tag{61}$$

$$\alpha_1 = \Delta t \tag{62}$$

$$\alpha_2 = \frac{\cosh(2\omega\Delta t) - 1}{4\omega^2} \tag{63}$$

$$\alpha_3 = \frac{\sinh(2\omega\Delta t) - 2\omega\Delta t}{8\omega^3}. \tag{64}$$

Matrix $\mathbf{A}$ is given by

$$\mathbf{A} = \begin{bmatrix} 0 & 1 & 0 & 0 \\ 0 & 0 & 0 & -1 \\ 0 & 0 & 0 & 0 \\ 0 & -4\omega^2 & -1 & 0 \end{bmatrix} \tag{65}$$

and its state transition matrix is given by

$$\mathbf{\Phi}(\Delta t) = \begin{bmatrix} 1 & \Delta t + 4\omega^2\alpha_3 & \alpha_3 & -\alpha_2 \\ 0 & 1 + 4\omega^2\alpha_2 & \alpha_2 & -\Delta t - 4\omega^2\alpha_3 \\ 0 & 0 & 1 & 0 \\ 0 & -4\omega^2\Delta t - 16\omega^4\alpha_3 & -\Delta t - 4\omega^2\alpha_3 & 1 + 4\omega^2\alpha_2 \end{bmatrix}. \tag{66}$$

The state transition matrix for the minus V-bar approach (which is used by ATV and some Russian vehicles) is also given by Eq. (66). To implement the algorithm the inverse of the top-right component of $\mathbf{\Phi}(\Delta t)$ is also needed, for the V-bar approach this inverse is given by

$$\mathbf{\Phi}_{r\lambda}^{-1}(\Delta t) = \frac{1}{-\alpha_3(\Delta t + 4\omega^2\alpha_3) + \alpha_2^2} \begin{bmatrix} -\Delta t - 4\omega^2\alpha_3 & \alpha_2 \\ -\alpha_2 & \alpha_3 \end{bmatrix}. \tag{67}$$

The R-bar approach consists in going to the ISS from below and it is used by HTV and Cygnus. Matrix $\mathbf{A}$ is given by

$$\mathbf{A} = \begin{bmatrix} 0 & 1 & 0 & 0 \\ 3\omega^2 & 0 & 0 & -1 \\ 0 & 0 & 0 & -3\omega^2 \\ 0 & -4\omega^2 & -1 & 0 \end{bmatrix}, \tag{68}$$

its eigenvalues are $\pm\omega$ and $\pm 3\omega$, the coefficients are given by

$$\alpha_0 = \frac{-\cosh(3\omega t) + 9\cosh(\omega t)}{8} \tag{69}$$

$$\alpha_1 = \frac{-(1/3)\sinh(3\omega t) + 9\sinh(\omega t)}{8\omega} \tag{70}$$

$$\alpha_2 = \frac{\cosh(3\omega t) - \cosh(\omega t)}{8\omega^2} \tag{71}$$

$$\alpha_3 = \frac{\sinh(3\omega t) - 3\sinh(\omega t)}{24\omega^3} \tag{72}$$

and the state transition matrix is

$$\mathbf{\Phi}(\Delta t) = \begin{bmatrix} \alpha_0 + 3\omega^2\alpha_2 & \alpha_1 + 7\omega^2\alpha_3 & \alpha_3 & -\alpha_2 \\ 3\omega^2\alpha_1 + 21\omega^4\alpha_3 & \alpha_0 + 7\omega^2\alpha_2 & \alpha_2 & -\alpha_1 - 10\omega^2\alpha_3 \\ 36\omega^6\alpha_3 & 12\omega^4\alpha_2 & \alpha_0 + 3\omega^2\alpha_2 & -3\omega^2\alpha_1 - 21\omega^4\alpha_3 \\ -12\omega^4\alpha_2 & -4\omega^2\alpha_1 - 40\omega^4\alpha_3 & -\alpha_1 - 7\omega^2\alpha_3 & \alpha_0 + 7\omega^2\alpha_2 \end{bmatrix}. \tag{73}$$

Finally the inverse of the top right component of the state transition matrix is given by

$$\mathbf{\Phi}_{r\lambda}^{-1}(\Delta t) = \frac{1}{-\alpha_3(\Delta t + 10\omega^2\alpha_3) + \alpha_2^2} \begin{bmatrix} -\alpha_1 - 10\omega^2\alpha_3 & \alpha_2 \\ -\alpha_2 & \alpha_3 \end{bmatrix}. \tag{74}$$

GUIDANCE LAWS COMPARISON

The first question we want to answer is whether the Space Shuttle V-bar approach is optimal under some condition. Once again, for the purpose of this discussion we ignore the canting of the orbiter's jets. The Shuttle's approach starts around 300 ft on the V-bar with a prescribed range rate at docking of 0.1 ft/s. Therefore glideslope's nominal trajectory is a constant-rate approach at 0.1 ft/s lasting 3000 seconds. Fig. 1 shows a comparison of the range profile of a vehicle being guided by glideslope and by the optimal guidance law. The figure shows that while for glideslope the range changes linearly, the optimal solution aquires In both cases the guidance law is called each second and is driven by perfect navigation. In all the examples the simulation uses nonlinear dynamics assuming central gravity only. The total integrated acceleration for the glideslope trajectory is 0.9433

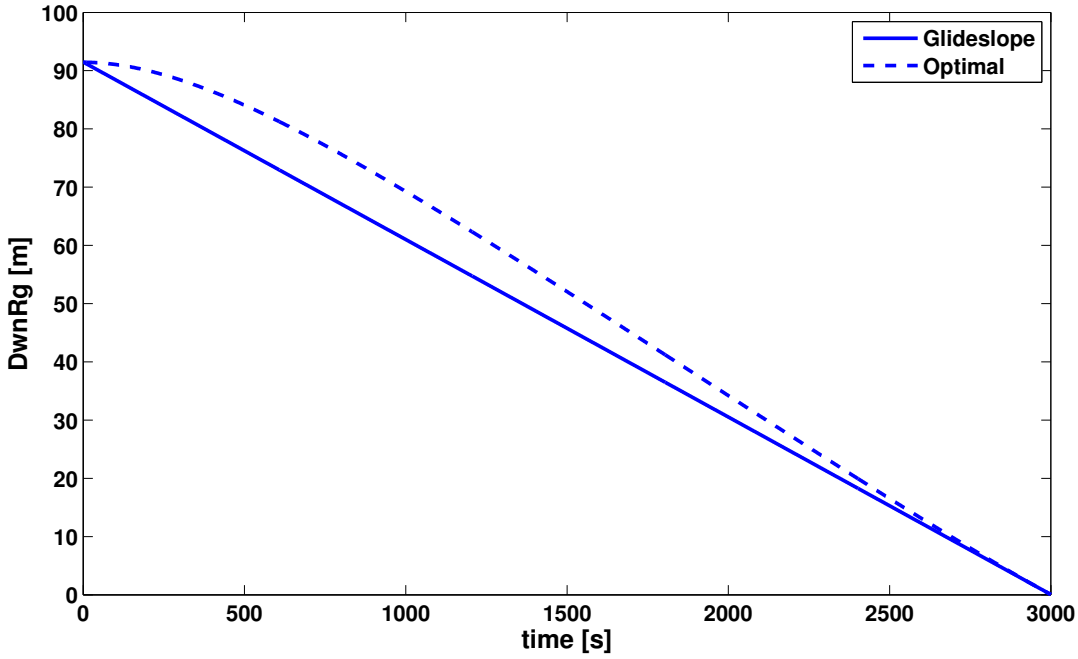

Figure 1. Comparison of V-bar Approaches

mm/s^2 and 0.0168 mm/s^2 for the optimal solution. However the Shuttle does not use low-thrust, therefore total delta-V is a more appropriate performance index. The total delta-V required to fly the glideslope trajectory is 0.2372 m/s, while the optimal solution requires 0.2235 m/s, a 5.78% improvement. The above scenario assumes the vehicle is placed on the V-bar with zero relative velocity. In the situation in which the vehicle is placed there with an initial 0.1 ft/s closing velocity the solutions of the two guidance laws coincide. While the Space Shuttle could be placed on the V-bar with a specefied velocity, the same strategy cannot be applied to other vehicles. The Cygnus vehicle [16], for example, needs to come to a stop at 250 m on the R-bar, and wait there until it obtains

authority to proceed from the ground. Therefore the approach starts from a zero relative velocity state. When this type of R-bar approach is simulated (with 15 m final range and zero final range rate) the total integrated velocity is 0.24 m/s^2 for glideslope and 0.0012 m/s^2 for the optimal solution. However this fact does not translate into better performance when high-thrust is used, since the optimal solution requires a total delta-V of 1.187 m/s while glideslope requires only 1.021 m/s. That comparison is done using a transfer time of 1791 s for the optimal solution, which coincides with the glideslope transfer time (which is not specifiable).

CONCLUSIONS

A common approach for the final phase of spacecraft rendezvous is to approach the target along a straight line, the so-called glideslope. In this paper a new fixed terminal direction guidance law to rendezvous with a target vehicle in circular orbit is introduced. The guidance law is derived by minimizing a commonly employed performance index that assumes finite thrust and is particularly adapt for electric thrusters. The guidance law is provided in closed-form assuming the vehicle starts from the glideslope. Calculation of a matrix exponential is required to compute the optimal acceleration. By performing some of the calculations *a priori* the total computational cost can be greatly reduced. For some commonly-employed glideslope angles the matrix exponential can be written analytically which allows for further reduction of the onboard computations.

The guidance law is obtained in closed-form by employing linearized dynamics, numerical examples demonstrate the validity of this assumption. A fixed direction approach requires continuous thrust and is less efficient than other approach strategies. For this reason this kind of guidance law is only used at the very end of the rendezvous phase when the vehicles are in close proximities and the linearization assumptions provide a very good approximation.

The proposed guidance law is compared to the another fixed-direction guidance law called glideslope.

REFERENCES

[1] Clark, F. D., Spehar, P. T., Brazzel, J. P., and Hinkel, H. D., "Laser-Based Relative Navigation and Guidance for Space Shuttle Proximity Operations," *Proceedings of the 26th Annual AAS Guidance and Control Conference*, Breckenridge, CO, February 5–9 2003, pp. 521–529.

[2] Pearson, D. J., "The Glideslope Approach," *Advances in the Astronautical Sciences*, Vol. 69, 1989, pp. 1145–1150, AAS 89-162.

[3] Ueda, S., Kasai, T., and Uematsu, H., "HTV Rendezvous Technique and GN&C Design Evaluation Based on 1st Flight On-orbit Operation Result," *Proceedings of the AIAA/AAS Astrodynamics Specialist Conference*, 2–5 August 2010, Toronto, Canada, AIAA-2010-7664.

[4] Ganet-Schoeller, M., Bourdon, J., and Gelly, G., "Non linear and Robust Stability Analysis for ATV Rendezvous Control," *Proceedings of the AIAA/AAS GN&C Conference*, 10–13 August 2009, Chicago, Illinois, AIAA-2009-5951.

[5] Miotto, P., Breger, L., Mitchell, I., Keller, B., and Rishikov, B., "Designing and Validating Proximity Operations Rendezvous and Approach Trajectories for the Cygnus Mission," *Proceedings of the AIAA/AAS GN&C Conference*, 2–5 August 2010, Toronto, Canada, AIAA-2010-8446.

[6] Lawden, D. F., *Optimal Trajectories for Space Navigation*, Butterworths, London, 1963, Chapter 5.

[7] Carter, T. E., "Fuel-Optimal Maneuvers of a Spacecraft Relative to a Point in Circular Orbit," *Journal of Guidance*, Vol. 7, No. 6, November–December 1984, pp. 710–716.

[8] Clohessy, W. H. and Wiltshire, R. S., "Terminal Guidance System for Satellite Rendezvous," *Journal of the Aerospace Sciences*, Vol. 27, September 1960, pp. 653–658.

[9] Lembeck, C. A. and Prussing, J. E., "Optimal Impulsive Intercept with Low-Thrust Rendezvous Return," *Journal of Guidance, Control, and Dynamics*, Vol. 16, No. 3, May–June 1993, pp. 426–433.

[10] Carter, T. E. and Humi, M., "Fuel-Optimal Rendezvous Near a Point in General Keplerian Orbit," *Journal of Guidance*, Vol. 10, No. 6, November–December 1987, pp. 567–573.

[11] Carter, T. E., "Optimal Power-Limited Rendezvous for Linearized Equations of Motion," *Journal of Guidance, Control, and Dynamics*, Vol. 17, No. 5, September–October 1994, pp. 1082–1086.

[12] Carter, T. E. and Pardis, C. J., "Optimal Power-Limited Rendezvous with Upper and Lower Bounds on Thrust," *Journal of Guidance, Control, and Dynamics*, Vol. 19, No. 5, September–October 1996, pp. 1124–1133.

[13] Guelman, M. and Aleshin, M., "Optimal Bounded Low-Thrust Rendezvous with Fixed Terminal-Approach Direction," *Journal of Guidance, Control, and Dynamics*, Vol. 24, No. 2, March–April 2001, pp. 378–385.

[14] Pardis, C. J. and Carter, T. E., "Optimal Power-Limited Rendezvous with Thrust Saturation," *Journal of Guidance, Control, and Dynamics*, Vol. 18, No. 5, September–October 1995, pp. 1145–1150.

[15] Hull, D. G., *Optimal Control Theory for Applications*, Springer, New York, 2003, Chapter 10.

[16] Miotto, P., Breger, L., Mitchell, I., Keller, B., and Rishikof, B., "Designing and Validating Proximity Operations Rendezvous and Approach Trajectories for the Cygnus Mission," *AIAA 2010-8446*, 2010.